J Mater Sci (2011) 46:1628–1634
DOI 10.1007/s10853-010-4978-2

Effects of high magnetic fields on solidification microstructure of Al–Si alloys

Tie Liu · Qiang Wang · Hong-Wei Zhang · Chang-Sheng Lou · Keiji Nakajima · Ji-Cheng He

Received: 15 June 2010 / Accepted: 4 October 2010 / Published online: 22 October 2010

Abstract The effects of high magnetic fields on the solidification microstructure of Al–Si alloys were investigated. Al–7.2 wt%Si and Al–11.8 wt%Si alloys were solidified in various high magnetic fields at different cooling rates. The secondary dendrite arm spacing (SDAS) of the primary Al dendrites and the lamellar spacing (LS) of the eutectics were measured. It was found that the application of a high magnetic field could decrease the SDAS of the primary Al dendrites in Al–7.2 wt%Si alloys and the LS of the eutectics in Al–11.8 wt%Si alloys. The effects of the high magnetic field on the SDAS decreased with increasing cooling rate. The decrease in the SDAS and LS can be attributed to the decrease of the solute diffusivity in the liquid ahead of the solid/liquid interface during the growth of the dendrite and eutectic. This decrease is caused by the high magnetic field which can damp the convection and avoid its contributions to the diffusion.

Introduction

The control of microstructure formation during solidification is becoming increasingly important for a wide variety of technical and scientific applications because a strong relationship exists between the performances of a material and its microstructure [1–4]. Recently, solidification processes in high magnetic field have been an extremely attractive and rapidly expanding research field due to the unique non-conducting feature that high magnetic fields affect the processes [5–7].

Many studies concerned with the effects of a magnetic field on solidification processes of materials have been reported till now. It has been recognized that the application of a magnetic field produces a Lorentz force on the moving electroconducting fluid. Because such Lorentz force has a nature of attenuating the movement of the fluid, the magnetic field has been used to modify some convection-relative processes during the solidification of semiconductor and metallic materials. For example, in the early classic work of Utech and Flemings [8], the solute bands in indium antimonide crystals caused by the temperature fluctuations in the melt ahead of the solid/liquid interface were eliminated by a magnetic field. Yasuda et al. [9] applied a high magnetic field to the unidirectional solidification of an Al–In monotectic alloy and produced a coupled growth between the solid Al and liquid In by reducing the local flow and fabricated an aligned rod structure. Zhang et al. [10] used a magnetic field to reduce the forced convection in electromagnetically levitated Cu–Co bulk samples and obtained a singular droplet size distribution of the Cu-rich minority phase. Li et al. [11] reported that the application of a magnetic field to the chill casting of an Al–Zn alloy induced a transformation of the microstructure from a mixture of equiaxed and columnar grains to twinned lamellar feathery grains. Such transformation was linked to the changes in the heat discharge and solute mixing. Another phenomenon of current interest is the effect of high magnetic field on the crystal orientation

T. Liu · Q. Wang (✉) · H.-W. Zhang · C.-S. Lou · K. Nakajima · J.-C. He
Key Laboratory of Electromagnetic Processing of Materials (Ministry of Education), Northeastern University, 110004 Shenyang, China
e-mail: wangq@epm.neu.edu.cn

K. Nakajima
Division of Applied Process Metallurgy, Department of Materials Science and Engineering, Royal Institute of Technology (KTH), 100 44 Stockholm, Sweden

of materials with anisotropy in the magnetic susceptibility. de Rango et al. [12] produced a highly oriented $YBa_2Cu_3O_7$ material using a solidification process in a high magnetic field and proved the possibility of magnetic crystal orientation at high temperature. Using the similar process, the magnetically oriented structures were also obtained in some metallic materials such as Bi–Mn [13, 14] and Al–Ni [15] alloys from either a melting [13, 15] or semi-solid state [14]. On the other hand, by applying a high magnetic field to a slow solidification process, the primary phases of certain alloys were found to align either parallel or perpendicular to the magnetic field direction [15–19]. Such phase alignment has been attributed to the combination of magnetic crystal orientation with other crystal growth-relative factors such as solute distribution [15], preferred crystallographic direction [15, 18], heat flow direction [18], and interaction between crystals [17, 19]. At the same time, the reports of the effects of high magnetic field gradients on solidification processes reveal a further application of high magnetic fields. Some of the present authors [19–22] illustrated that the distributions of the primary phases or alloying elements of some alloys and their solidification microstructures could be controlled in terms of magnetic force by high magnetic field gradients. For instance, the primary MnBi grains in a hypereutectic Bi–Mn alloy were driven by the magnetic force to migrate in the liquid matrix during solidification and form a microstructure of which the MnBi grains exhibited a gradient distribution [19], whereas the Mn element in near eutectic Mn–Sb alloys were separated prior to the solidification to form a Mn- and Sb-rich regions in the both sides of the melt and create the coexistence of both primary MnSb and Sb phases in specimen with a continuous change in their volume fractions [21, 22].

These initial studies suggested that applying a high magnetic field during solidification processes offers an opportunity to in situ control the microstructure of metallic materials. Thus, the understanding of the relationship between microstructural evolution of these materials during solidification and the high magnetic field would lead to a better understanding of how to realize such control. This study was conducted to gain further understanding about the effects of high magnetic fields on the solidification processes of metallic materials and its dependence on processing parameters such as cooling rate. The microstructural evolution, especially the changes in secondary dendrite arm spacing (SDAS) of the primary Al dendrites, and lamellar spacing (LS) of the eutectics, in Al–Si alloys solidified in various high magnetic fields, were characterized by optical microscopy and an image analyzing system. The temperature behavior of the alloys during continuous cooling was also monitored by direct thermocouple measurements.

Experimental procedure

Two hypoeutectic Al–Si alloys were prepared by induction–melting together of Al with Si of 4 N high purity in high-pure graphite crucibles in a dynamic Ar atmosphere. The alloy compositions were chemically analyzed to be 7.2 and 11.8 wt%Si. The obtained ingots were then machined into cylindrical specimens 9.5 mm in diameter and 15 mm in length.

The specimens were placed onto alumina crucibles (inner diameter 10 mm; outer diameter 15 mm) and heated in an Ar atmosphere to temperatures which were approximately 150 °C higher than their liquidus temperatures at a heating rate of 5 °C/min. After holding at the same temperature for 30 min, the specimens were cooled down to 500 °C at different cooling rates. Finally, the specimens were cooled down to room temperature within about 60 min by turning off the DC power source. The specimens were also solidified in the presence of various high magnetic fields. The experimental conditions are summarized in Table 1. Details of the experimental apparatus have been reported previously [23]. The temperature/time curves were obtained by inserting a Pt–13%Rh thermocouple, which was contained in an alumina sheath (inner diameter 2 mm; out diameter 3 mm), into the specimens through the bottom of the crucibles, as shown in Fig. 1. The output from the thermocouple was continuously recorded at 0.5-s intervals. The thermocouple was standardized against the melting point of pure aluminum specimens, which gave arrests at 660 ± 0.2 °C under the same experimental conditions. Note that the presence of the high magnetic field does not influence the temperature measurement; the current experimental method can allow sufficiently precise measurements.

After the solidification, the specimens were cut along the plane either parallel or perpendicular to the imposed magnetic field direction and prepared for metallographic examination using standard metallographic procedures. The SDAS of the primary Al dendrites in the Al–7.2 wt%Si alloy specimens and the LS between parallel eutectic Si in the Al–11.8 wt%Si alloy specimens were measured using an image analyzing system. The measurement method used was the combination of line intercept and individual arm counting methods [24, 25]. For the

Table 1 Experimental conditions for the solidification of Al–Si alloys

Alloy composition (wt%Si)	Magnetic flux density (T)	Cooling rate (°C/min)
7.2	0, 8.8	1.5, 10, 15
11.8	0, 4.4, 8.8, 11.5	1.5

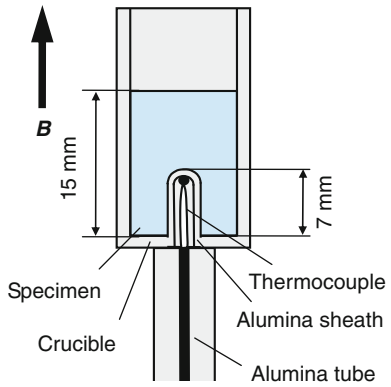

Fig. 1 Schematic view of the assembly for in situ temperature measurement in high magnetic fields

former, above 30 values were measured and averaged for each specimen, whereas for the latter, above 70 values were measured and averaged for each specimen.

Experimental results

Figure 2 shows the typical as-cast microstructures of Al–7.2 wt%Si alloys solidified with and without a high magnetic field of 8.8 T at cooling rates of 1.5, 10, and 15 °C/min (these cooling rates have been confirmed by the cooling curves measured by a thermocouple). Because of the relatively smaller cooling rates adopted in this study (≤15 °C/min), the morphology of the primary Al is predominantly dendritic. It is evident from the figure that with the increase in the cooling rate, the primary Al dendrites are strongly refined. In the alloys solidified at 10 and 15 °C/min, the dendrites are well developed with secondary arms and dendrite tips becoming clearly visible. On the basis of these microstructures, the SDAS of the primary Al dendrites was measured. The measurement results with associated errors are shown in Fig. 3 as a function of the cooling rate. It can be seen that for both cases of with and without the magnetic field, the SDAS decreases with increasing cooling rate. Such decrease can be clearly observed in the microstructures as shown in Fig. 2. The comparison between the cases of with and without the magnetic field shows that the SDAS is decreased by the application of the magnetic field. However, such decrease in the SDAS induced by the magnetic field becomes less pronounced with the increase in the cooling rate.

For Al–11.8 wt%Si alloys, also because of the relatively lower cooling rate of 1.5 °C/min, the eutectic Si in all experimental conditions exhibits an irregular lamellar-like morphology. A careful examination on the morphology of the eutectic Si shows that the application of the high magnetic field does not obviously affect the shape orientation of the eutectic Si on both the longitudinal and transverse sections. The eutectic Si still shows a random distribution. Because the LS strongly depends on the angle of the measured lamellas with the observed surface of the specimens, the LS of the eutectic Si on both the longitudinal and transverse sections was measured and compared. The comparison results show that there is no obvious difference between the average LS values obtained from these two sections. Therefore, the LS was determined by averaging all measurements conducted on both sections. Figure 4 shows typical microstructures of the eutectics in Al–11.8 wt%Si alloys on the longitudinal section solidified under various magnetic field conditions. The LS measurement results with associated errors are shown in Fig. 5 as a function of the magnetic flux density. It can be seen that the LS of the eutectic Si is decreased by the application of the magnetic fields, but the increase in the magnetic flux density does not bring additional effect on the LS. Furthermore, it can be seen from the errors that the application of the magnetic fields produces a more uniform distribution of the LS.

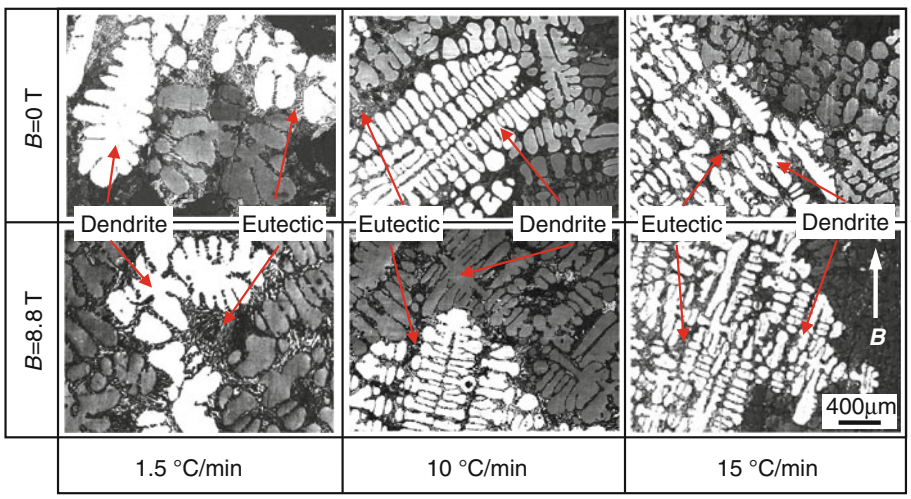

Fig. 2 Typical microstructures indicating that the eutectics are distributed at the grain boundaries of the primary Al dendrites in Al–7.2 wt%Si alloys solidified with and without a high magnetic field of 8.8 T at cooling rates of 1.5, 10, and 15 °C/min

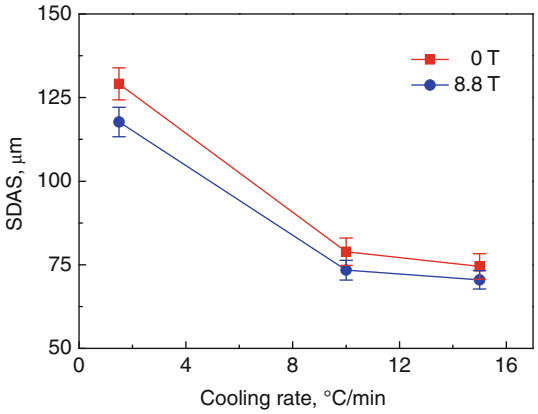

Fig. 3 SDAS of the primary Al dendrites in Al–7.2 wt%Si alloys solidified with and without a magnetic field of 8.8 T as a function of the cooling rate

Discussion

The SDAS measurement results have indicated that the application of the high magnetic field can decrease the SDAS of the primary Al dendrites. Based on extensive experimental studies and theoretical analyses [26, 27], the SDAS (λ_2) has been linked to solute chemical diffusivity in the liquid (D) and tip growth rate (R), and is given by

$$\lambda_2 = M\left(\frac{D}{R}\right)^{2/3} \quad (1)$$

where M is a factor and depends on alloy composition, solute partition coefficient, and fusion temperature of the solvent. Previous studies on the effects of a high magnetic field on the chill casting process of an alloy have suggested that the thermal exchange between the alloy and the environment could be reduced by the magnetic field through suppressing the convection in the melt [11]. However, in this study the cooling of the alloys was carefully controlled, the heat extraction from the alloys was therefore not obviously altered by the imposed magnetic fields. This has been evidenced by the cooling curves directly measured by the thermocouple during the solidification of the alloys, as shown in Fig. 6. In the curves, all alloys do not show obvious undercooling in spite of the use of a large overheating. This indicates that the nucleation of those dendrites is triggered by heterogeneous nuclei [28, 29]. For hypoeutectic Al–Si alloys, these nuclei can mostly be oxides [30]. It can be seen from the figure that the cooling rates for the primary reaction of the alloys of both with and without the magnetic field cases do not show obvious difference. Thus, a conclusion can be deduced that the application of the high magnetic field exhibits a negligible effect on the tip growth rate in this study. Furthermore, these cooling curves also indicate that a high magnetic field of 8.8 T has no obvious effect on the phase equilibria of the Al–Si system. This has been confirmed by the temperature measurement results published by Aoki et al. [31]. Thus, these parameters relative to the factor M of Eq. 1 should not change obviously. Consequently, the decrease in the SDAS in the magnetic field can be mainly attributed to the change in the solute diffusivity. In liquids, mass transport can be significantly enhanced by different types of convection. There then arises the assumption that the solute diffusion in a melt may be reduced by a high

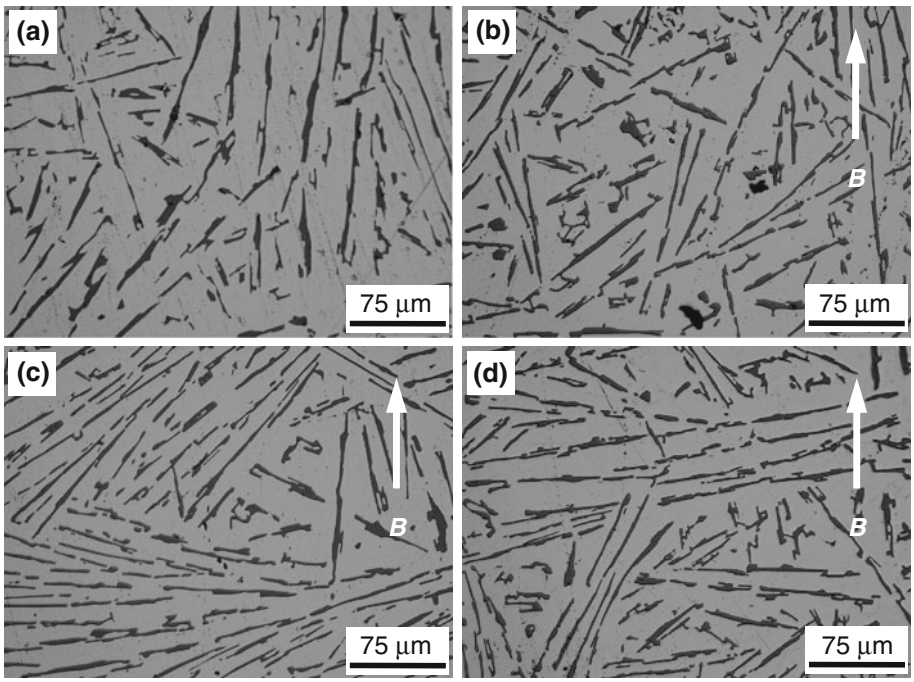

Fig. 4 Typical microstructures of the eutectics in Al–11.8 wt%Si alloys solidified at a cooling rate of 1.5 °C/min under various magnetic field conditions. **a** $B = 0$ T; **b** $B = 4.4$ T; **c** $B = 8.8$ T, and **d** $B = 11.5$ T

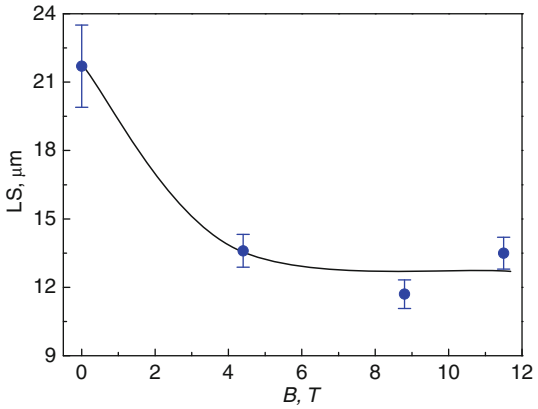

Fig. 5 LS of the eutectic Si in Al–11.8 wt%Si alloys solidified at a cooling rate of 1.5 °C/min as a function of the magnetic flux density

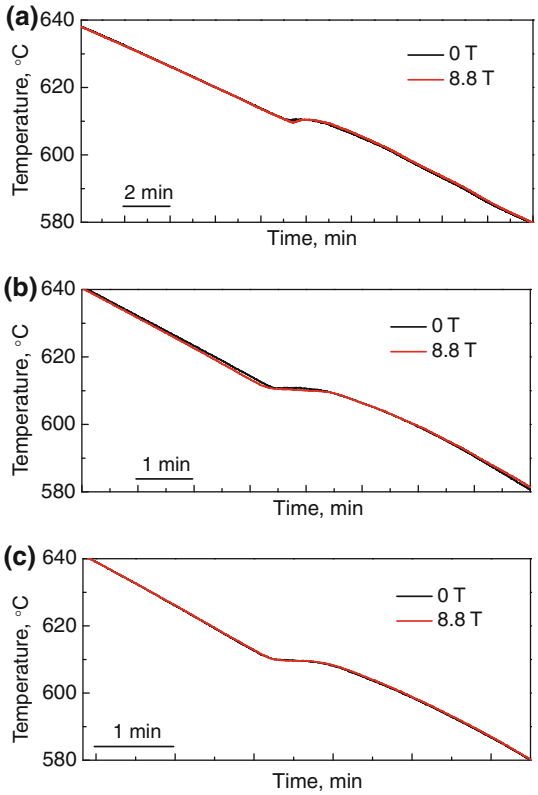

Fig. 6 Cooling curves for the primary reactions of Al–7.2 wt%Si alloys solidified with and without an 8.8 T magnetic field at cooling rates of **a** 1.5, **b** 10, and **c** 15 °C/min

magnetic field because the Lorentz force induced by the magnetic field can damp the motion of the melt. In fact, this assumption has been confirmed by the results of several previous studies [32–34]. Mathiak and Frohberg [32] reported that the interdiffusion between liquid In and Sn in a capillary was reduced by a magnetic field to the magnitude of that obtained in microgravity. Using a shear cell method, Botton et al. [33] obtained the similar results from the diffusion couple of Sn–SnIn (1 at.%) and Sn–SnBi (0.5 at.%). Their calculations also showed that a magnetic field around 2.5 T would high enough to avoid the contributions of the convection to the diffusion in most of liquid metals. Some of the present authors [34] investigated the diffusion behavior of liquid/solid (Al/Cu) couples in a high magnetic field and observed a decrease in the thickness of the diffusion layer resulted from the absence of the convection in the liquid phase. Therefore, the application of the high magnetic field to the growth of the primary Al dendrites should weaken the diffusion of Si from the enriched boundary layer ahead of the solid/liquid interface by suppressing the convection. According to Eq. 1, the SDAS of the primary Al dendrites will be decreased accordingly.

Our experimental results have shown that the high magnetic field exhibited a decreasing effect on the SDAS of the primary Al dendrites with increasing cooling rate. Equation 1 has indicates that the SDAS is strongly dependent on the tip growth rate, as well as on the solute diffusivity. With the increase in the cooling rate, the mean tip growth rate should be increased simultaneously, resulting in a decrease in the SDAS. In this way, there will be a competition between the effects of the magnetic field and the cooling rate on the SDAS. According to Eq. 1, when the tip growth rate (cooling rate) is small, the SDAS is mainly controlled by the solute diffusivity and the change in the solute diffusivity can induce obvious change in the SDAS. However, when the tip growth rate (cooling rate) is large, the SDAS will be mainly controlled by the tip growth rate and the change of the solute diffusivity will show a less obvious effect on the SDAS. Therefore, the decreasing effect of the high magnetic field on the SDAS with increasing cooling rate can be attributed to that the decrease in the SDAS induced by the high magnetic field was not compared with the increase in the SDAS induced by the increase in the cooling rate. In this study, the magnetic field of 8.8 T could still exhibit an observable effect on the SDAS at a cooling rate up to 15 °C/min. It is however expected that the magnetic field will no longer obviously affect the SDAS when the cooling rate is high enough.

Except for the effect on the SDAS of the primary Al dendrites, the high magnetic field was also found to decrease the LS of the eutectic Si of the Al–Si alloys. A modified Jackson–Hunt model has been established to describe the growth of irregular eutectic such as Al–Si eutectic [35, 36]. In this model, similar to the model used to describe the growth of the dendrite (Eq. 1), the average LS (λ_a) has been linked to solute diffusivity in the liquid (D) and growth rate (V), and is given by

$$\lambda_a = N\left(\frac{D}{V}\right)^{1/2} \quad (2)$$

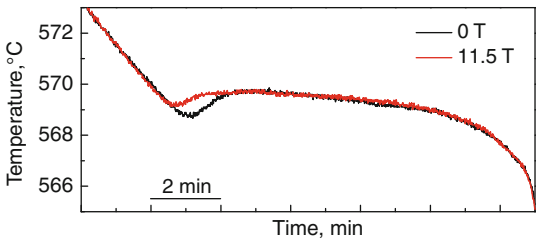

Fig. 7 Cooling curves for the eutectic reaction of Al–11.8 wt%Si alloy solidified with and without an 11.5 T magnetic field at a cooling rate of 1.5 °C/min

where N is a factor and can be evaluated by the phase diagram parameters and material properties of the concerning alloy system. As discussed above, the magnetic field of 8.8 T has no obviously effect on the phase equilibria of the Al–Si system and thus should not alter the factor N. The cooling curves for the eutectic reaction of Al–11.8 wt%Si alloys solidified with and without a magnetic field of 11.5 T at a cooling rate of 1.5 °C/min show that the magnetic field did not obviously affect the heat extraction from the alloys (Fig. 7). Thus, the mean growth rate of the eutectic Si should not be obviously altered by the magnetic field. From a series of cooling curves of the Al–11.8 wt%Si alloys solidified in various high magnetic fields, the application of the magnetic field was found to show a random effect on the recalescence of the curves. For instance, the recalescence was slightly decreased in the cooling curve as shown in Fig. 7 but slightly increased in some other cooling curves by the application of the magnetic field. Furthermore, such change in recalescence was not found to cause an obvious effect on the LS of the eutectic Si. Consequently, the decrease in the LS in the high magnetic fields can be attributed to the decrease in the solute diffusivity in the liquid ahead of the solid/liquid interface because of the damping of the convection in terms of the Lorentz force. The fact that the increase in the magnetic flux density did not bring additional effect on the LS (Fig. 5) indicates that the magnetic field of 4.4 T has been strong enough to completely suppress the convection in the Al–Si melt.

Conclusions

The effects of high magnetic fields on the solidification microstructure of Al–Si alloys were investigated. Al–7.2 wt%Si and Al–11.8 wt%Si alloys were solidified in various high magnetic fields at different cooling rates. The SDAS of the primary Al dendrites and the LS of the eutectics were examined by an image analyzing system. The cooling curves of the alloys during solidification process were measured by a thermocouple. It was found that the application of a high magnetic field could decrease the SDAS of the primary Al dendrites in Al–7.2 wt%Si alloys and the LS of the eutectics in Al–11.8 wt%Si alloys. The effect of the high magnetic field on the SDAS decreased with increasing cooling rate. The decrease in the SDAS and LS can be attributed to the decrease in the solute diffusivity in the liquid ahead of the solid/liquid interface during the growth of the dendrite and eutectic caused by the high magnetic field which can damp the convection and avoid its contributions to the diffusion.

Acknowledgement This study was supported by the National Natural Science Foundation of China (Grant No. 51006020), the Fundamental Research Funds for the Central Universities (Grant Nos. N090109001, N090209001), the Program for New Century Excellent Talents in University, People's Republic of China (Grant No. NCET-06-0289), and the 111 project (Grant No. B07015).

References

1. Liu F, Yang GC (2006) Int Mater Rev 51:145
2. Lavernia EJ, Srivatsan TS (2010) J Mater Sci 45:287. doi:10.1007/s10853-009-3995-5
3. Tavitas-Medrano FJ, Mohamed AMA, Gruzleski JE, Samuel FH, Doty HW (2010) J Mater Sci 45:641. doi:10.1007/s10853-009-3978-6
4. Zuo M, Liu XF, Sun QQ (2009) J Mater Sci 44:1952. doi:10.1007/s10853-009-3287-0
5. Asai S (2000) Sci Technol Adv Mater 1:191
6. Gillon P (2000) Mater Sci Eng A 287:146
7. Watanabe T, Tsurekawa S, Zhao X, Zuo L, Esling C (2006) J Mater Sci 41:7747. doi:10.1007/s10853-006-0740-1
8. Utech HP, Flemings MC (1966) J Appl Phys 35:2021
9. Yasuda H, Ohnaka I, Fujimoto S, Takezawa N, Tsuchiyama A, Nakano T, Uesugi K (2006) Scripta Mater 54:527
10. Zhang YK, Gao J, Nagamatsu D, Fukuda T, Yasuda H, Kolbe M, He JC (2008) Scripta Mater 59:1002
11. Li L, Zhang YD, Esling C, Zhao ZH, Zuo YB, Zhang HT, Cui JZ (2009) J Mater Sci 44:1063. doi:10.1007/s10853-008-3158-0
12. de Rango P, Lees M, Lejay P, Sulpice A, Tournier R, Ingold M, Germi P, Pernet M (1991) Nature 349:770
13. Morikawa H, Sassa K, Asai S (1998) Mater Trans JIM 39:814
14. Yasuda H, Ohnaka I, Yamamoto Y, Tokieda K, Kishio K (2003) Mater Trans 44:2207
15. Wang CJ, Wang Q, Wang ZY, Li HT, Nakajima K, He JC (2008) J Cryst Growth 310:1256
16. Mikelson AE, Karklin YK (1981) J Cryst Growth 52:524
17. Liu T, Wang Q, Zhang C, Gao A, Li DG, He JC (2009) J Mater Res 24:2321
18. Liu T, Wang Q, Gao A, Zhang C, Li DG, He JC (2009) J Alloys Compd 481:755
19. Wang Q, Lou CS, Liu T, Wei N, Wang CJ, He JC (2009) J Phys D 42:025001
20. Wang Q, Liu T, Gao A, Zhang C, Wang CJ, He JC (2007) Scripta Mater 56:1087
21. Liu T, Wang Q, Gao A, Zhang C, Wang CJ, He JC (2007) Scripta Mater 57:992
22. Liu T, Wang Q, Gao A, Zhang HW, Wang K, He JC (2010) J Mater Res 25:1718
23. Wang Q, Wang CJ, Liu T, Wang K, He JC (2007) J Mater Sci 42:10000. doi:10.1007/s10853-007-2050-7

24. Muojekwu CA, Samarasekera IV, Brimacombe JK (1995) Metall Mater Trans B 26:361
25. Hosch T, England LG, Napolitano RE (2009) J Mater Sci 44:4892. doi:10.1007/s10853-009-3747-6
26. Kirkaldy JS, Liu LX, Kroupa A (1995) Acta Metall Mater 43:2905
27. Bouchard D, Kirkaldy JS (1997) Metall Mater Trans B 28:651
28. Tournier RF (2007) Physica B 392:79
29. Tournier RF, Beaugnon E (2009) Sci Technol Adv Mater 10:014501
30. Turnbull D, Cech RE (1950) J Appl Phys 21:804
31. Aoki Y, Hayashi S, Komatsu H (1992) J Cryst Growth 123:313
32. Mathiak G, Frohberg G (1999) Cryst Res Technol 34:181
33. Botton V, Lehmann P, Bolcato R, Moreau R, Haettel R (2001) Int J Heat Mass Transfer 44:3345
34. Li DG, Wang Q, Liu T, Li GJ, He JC (2009) Mater Chem Phys 117:504
35. Magnin P, Trivedi R (1991) Acta Metall Mater 39:453
36. Magnin P, Mason JT, Trivedi R (1991) Acta Metall Mater 39:469